

Biological Nano-crystallization

- ▶ [Macromolecular Crystallization Using Nanovolumes](#)

Biological Photonic Structures

- ▶ [Structural Color in Animals](#)

Biological Platform

- ▶ [Biological Breadboard Platform for Studies of Cellular Dynamics](#)

Biological Sensors

- ▶ [Arthropod Strain Sensors](#)

Biological Structural Color

- ▶ [Structural Color in Animals](#)

BioMEMS/NEMS

- ▶ [Nanotechnology](#)

Biomimetic Antireflective Surfaces Arrays

- ▶ [Moth-Eye Antireflective Structures](#)

Biomimetic Energy Conversion Devices

- ▶ [Self-repairing Photoelectrochemical Complexes Based on Nanoscale Synthetic and Biological Components](#)

Biomimetic Flow Sensors

Jérôme Casas¹, Chang Liu² and Gijs Krijnen³

¹Institut de Recherche en Biologie de l'Insecte, IRBI UMR CNRS 6035, Université of Tours, Tours, France

²Tech Institute, Northwestern University, ME/EECS, Room L288, Evanston, IL, USA

³Transducers Science & Technology group, MESA + Research Institute for Nanotechnology, University of Twente, Enschede, The Netherlands

Definition

Biomimetic flow sensors are biologically inspired devices that measure the speed and direction of fluids.

Introduction

This survey starts by describing the role and functioning of airflow-sensing hairs in arthropods and in fishes, carries on with the biomimetic MEMS implementations, both for air and water flow sensing, and ends up with some perspectives for bio-inspired micro-technologies based on the latest understanding of the biological sensors.

Inspiring Biological Systems

Flow sensing systems have been mainly studied on crickets and cockroaches, and to a lesser degree on spiders. The fact that the latter are predators of the former seems to matter little so far, and this entry will concentrate on the cricket for comprehensiveness. Flow sensors in crustaceans living in water have been studied to an even lesser degree but in a similar fashion, without any relationship with biomimetics, so that these works are not mentioned here.

Arthropod Hairs

The filiform hairs of many insects, spiders, and other invertebrates are among the most delicate and sensitive flow sensing cells: they measure displacements on the order of a fraction of the hydrogen atomic diameter (sensitivity ca. 10^{-10} m = 1 Å) and react to flow speeds down to 30 μm/s. If one considers the energy needed to elicit a neuronal spike, one finds that they react with a thousandth of the energy contained in a photon, so that they surpass photoreceptors. In fact, these mechanoreceptors work at the thermal noise level [19]. These hairs pick up air motion, implying that they are measuring both the direction and speed of air particles, in contrast to pressure receivers, i.e., ears. Many insects have ears, so that the extra information available in the flow field must be useful. The biomechanics of the filiform hairs have been studied with care since several decades by several groups worldwide, based on the analogy with a single degree of freedom inverted pendulum without bending (see the latest review of hair biomechanics in [8]).

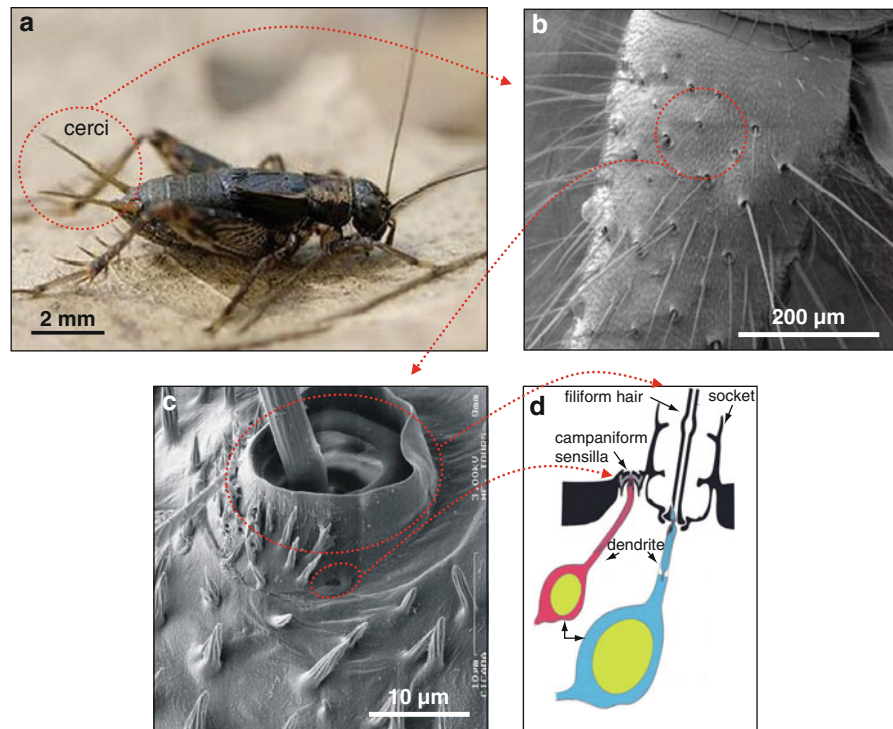
Among insects, mainly cockroaches and crickets have been studied, because their airflow-sensitive hairs are put on two antenna-like appendages, the cerci (cercus in singular, see Fig. 1). Insect hairs have usually a high aspect ratio, with a length of a few hundreds of microns up to 2 mm, and with a diameter of less than a dozen of microns (Fig. 1). Their tapered shape have been found to have an influence on the drag forces. Hairs and sockets are ellipsoidal in cross section, which leads to a movement in a preferred direction. The hairs of spiders, called trichobothria, are often curved, are innervated by several sensory cells and have an ultrastructure which is favorable to drag while minimizing weight (a feathery structure which decreases the mass and hence their inertia considerably, while increasing the friction in air). The studied airflow-sensing trichobothria are located on the legs. These two aspects regarding the exact form of cricket and spider hairs show that natural selection is acting on the tiniest details of biological organization. The base of the hairs is much more complex, and its mechanics poorly understood. In crickets, only a single sensory cell is below the hair shaft, while spiders have several (Fig. 1). At the base of the socket, another mechanoreceptor type, the campaniform sensilla, reacts to deformation of the cuticula produced by the movement of the socket. Crickets possess often two

sensilla around each hair. Thus the two sensors types act as a coupled system, extending thereby the range of forces it can measure.

Arthropods are very often quite hairy, and the high density of flow sensing hairs implies that they interact with each other in order to produce a high-resolution map of flow characteristics, acting like a flow camera (Fig. 1). Up to now, only the hydrodynamic type of interaction has been studied, called viscous coupling. It was found to be highly dependent on the geometrical arrangement of hairs, of their respective lengths and preferential planes of movement, as well as on the frequency content of the input signal [4]. Hairs often interact over long distances, up to 50 times their radius, and usually negatively. Short hairs in particular “suffer” substantially from the presence of longer hairs nearby, due to a shadowing effect. Positive interactions, where the flow velocity at one hair is increased by the presence of nearby hairs, have been however observed in real animals and reproduced computationally. The biological implications of these interactions have only very recently been addressed, and hint toward a coding of incoming signals which relies strongly on the specific sequence of hairs been triggered [16]. In other words, the signature of the incoming signal is mapped into a given sequence of recruited hairs, which in turn produces a typical sequence of action potentials.

Single hairs, or groups of hairs, are not placed at random on the body. For the same reasons that the exact shape of hairs and their relative position within a group have been most likely molded by natural selection, the position of the hairs on the sensory organ must be shaped by selection. This aspect of mechanosensory research is however badly neglected. As for the positions along the cercus, the presence of a potential acoustic fovea (i.e., a location with particularly high acuity) at the base of the cercus has been hinted already twice, not only due to the highest hair density in this region, but also because it corresponds to the region with the largest flow velocities, the cercus being the largest there. Putting hairs radially around the cercus enables crickets also to pick up transversal flows, whose peak flow velocities are larger than in the situation where the hairs would be placed on a flat surface; in the later case, hairs are submitted to longitudinal flow with lower peak velocities. In summary, where you put your sensors relative to your body geometry matters a lot.

Biomimetic Flow Sensors, Fig. 1 Habitus of a wood cricket (a), with the two cerci highlighted, on which a large number of filiform hairs, intermixed with spines and chemoreceptive hairs, can be observed (b). The socket of a hair is a complex system made of several membranous stoppers. Its deflection is sensed through another type of mechanosensor, the campaniform sensilla, which is a strain detector (c). Both act as a coupled system, the cuticula being deformed once the hair touches the border of the socket. Each sensor is innervated by a single hair cell (d)



An action potential triggered by a moving hair ends up directly in the terminal abdominal ganglion (TAG), a local neuronal processing unit. Information from all the hairs, as well as from other sensors, converges there and is processed by interneurons. The compression and convergence of information at this stage is huge: About 1,500 afferent neurons of hairs are connected to only some 20 interneurons [10]. The fact that invertebrates possess few large, singly identifiable neurons enabling comprehensive mapping and repeated recordings of activities is a unique asset which explains the interest in such exotic systems. Information coming from the central brain as well as from the higher ganglia also descends into the TAG. Once processed, the combined information moves up quickly toward higher neuronal centers, in particular the ganglia in which the hindleg movements are being decided. This local feedback loop, with little input from the main brain, enables the animal to process vital information and act accordingly very quickly. As so often with invertebrates, what can be processed locally should be done so, a distributed processing scheme which explains why biomimetics has so much to gain from this group of animals.

The last level of integration is behavior, and flow sensing is known to be of importance in predator and prey perception, sexual selection, and most likely other context, such as noticing its own speed and movement. Predator avoidance is obviously a major selection force, where speed is of paramount importance. Jumping or running away is the behavior which is elicited using appropriate stimuli. The cricket possesses in the TAG an internal map of the direction of the stimuli from the outside world and the geometric computation of the direction of incoming flow by the cercus is one of the nicest case studies of spatial representation [10]. Computing the speed of an approaching predator is also carried out by the TAG, and has been only recently established using appropriate stimuli. Where to jump is a different question, in which directing stimuli and other conditions intervene.

Natural selection therefore acts along the full chain of information transfer, from acquisition and processing, up to actuation. This is important to restate in a biomimetic context, as the extreme sensitivity on the biomechanical side of the hair shaft, which has been the exclusive focus of the engineer attention, could be otherwise lost into an inefficient sequence of

information transfer. As of today, one has however very little information about the constraints acting on the different parts of the chain, and hence no idea about their optimization levels.

Fish Neuromasts

Hair cells of the lateral-line system of fish are able to detect water displacement of the order of ca. 20 nm [2]. This ability is used in various ecological contexts, such as prey and predator localization, schooling, and most likely a host of other behaviors. Fish can also detect obstacle-created flow distortions of a flow field they have generated. The blind cave fish, *Astyanax fasciatus*, is an interesting model because it is believed that this species, having lost sight and having to maneuver in darkness, possesses particularly sensitive hair cells. The spatial discrimination ability, through self-induced water movements when approaching objects, of the blind cave fishes is about 1 mm². The hairs of fish are located within specialized units, called neuromasts. These neuromasts, which are localized in many different parts of the body and which do not display a strong correlation with the flow structure of their environments, are located either just on the skin (called superficial neuromasts), or in specialized fluid-filled canals which produce a reticulated pattern on the head and along the body sides. A single neuromast consists of sensory cells that project into a jelly-like material, the cupula, in which several hairs (or cilia) of different lengths are embedded. The cupula is therefore the medium which connects the hairs and the external fluid.

An Engineering Perspective on Biomimetic Hairs

Hair-based flow sensing systems of arthropods and fish contain various levels, ranging from the mechanical structure, to the generation of action potentials in neurons, and signal transport, collecting and processing signals from many (hair-) sensors in the various neuronal centers. Taking inspiration from such complex systems is a non-trivial endeavor. The mechanics of these sensory systems are relatively easy to mimic in an engineering context, at least in comparison to the complexity of the neural system which requires

delicate materials (e.g., membranes with ion-channels) and fluids with ion concentrations robustly and actively maintained by the organism. Consequently, up to date most of the bio-inspired flow sensors actually are defined merely by the fact that they use a hair, if needed covered by a cupula resembling cover, to capture viscous drag forces. Having no neural system in an engineering context implies that signal transduction, i.e., from the mechanical to the electrical domain, needs to be done by rather “un-bio-inspired” methods, e.g., using capacitive or piezoresistive interrogations methods. The next level up, namely the arrangement of the hair sensors into an array like structure (a cercal canopy for crickets and a lateral line for fish), is again open to engineering approaches. Mimicking the entire hair-based sensory system requires the ability to recreate dense hair-sensor arrays, including the associated electronic interfacing, asking for engineering solutions to the multiplexing problems. On the signal processing level, the biomimetic content can be high again, e.g., by exploitation of artificial neural networks to extract features and events from the multitude of array signals. The insight in the neuronal architecture of the animals needed for such exercise is however at best sketchy, with the exception of the architecture behind the directional acuity of crickets.

In view of the overall shape and sizes of the hairs in combination with the high densities and large numbers of hair sensors on the hair canopies, it is obvious that an artificial version of this kind of sensor arrays cannot be assembled but should be made monolithically. As it turns out, the range of dimensions is well attainable by micromachining techniques as used in the field of micro-electro-mechanical systems (MEMS). However, the materials generally used in MEMS are rather stiff compared to the materials found in nature, calling for some creative engineering.

Various types of hair-based flow sensors, for operation in air as well as in water, have been developed using both conventional machining and micromachining technologies. They are based on a variety of materials (including semiconductor, oxide, and polymers) and transduction principles (including electrostatic sensing, piezoresistive sensing, thermal sensing, etc.). However, artificial hair-cell (AHC) sensors represent unique challenges to microengineering design and fabrication. The high aspect ratio, vertical, hair must be fabricated using processing steps that are amenable to engineering,

manufacturing and eventually scaled production. The overall process must be scalable to large areas as the AHC sensors are often used in arrays. Ideally, the sensors should be integrated with highly sensitive transduction mechanisms to couple mechanical input to electrical output. Further, it is desirable that the AHC sensors be made on a substrate that also houses the integrated electronics elements for signal conditioning and amplification.

For reasons outlined above, most of the hair-based flow sensors reported in literature are made using MEMS fabrication technology. Ironically, the fabrication of the relative large hair structures poses considerable difficulties in this technology. Two basic types of artificial hairs can be distinguished, namely, hairs fabricated in the wafer plane and hairs fabricated perpendicular to the wafer plane. The first is straightforward since surface micromachining techniques can be used. However, surface-micromachined hairs cannot easily be combined into high-density arrays. An overview of the various reports in literature on ciliar inspired actuators and sensors is found in [22].

Ozaki et al. [17] were probably the first to provide flow sensors inspired by insects. Their piezoresistance-based sensors had either 400–800 μm long hairs in plane, being cantilevers exposed to flow after removing large part of the silicon substrate, or consisted of wires manually glued to a cross-shaped piezoresistive structure delivering two DOF sensitivity. Characterization by continuous flows in the m/s range proofed the functionality and directivity of the sensors. A comparable in-plane hair fabrication process was used in [12], but incorporated a stress gradient in the artificial hairs to make them curve out of plane. Readout is obtained by tracking the flow-induced vibrations of a set of dissimilar hairs resonating at different frequencies when exposed to specific flows. Argyrakis et al. [1] also use in-plane cantilevers with piezoresistive readout connected to an artificial neuronal circuit for spike generation. An alternative approach was proposed in [15] where the actual hair consisted of an optical fiber with reduced optical transmission when displaced by viscous drag. The sensor is meant for DC-flow measurements and achieves high volumetric sensitivity ($\mu\text{L}/\text{min}$ range). Xue et al. [20] more or less reverted to the structure of Ozaki using a cross-shaped frame with piezoresistors with a plastic hair of about 5 mm length. A nice twist on the hair

sensor is presented in [14] by exploiting piezoelectric transduction by polyvinylidene fluoride in thermo-direct written clamped–clamped beam-type structures. Recently, interesting results have been obtained using a straightforward cantilever design in combination with appropriate electronic feedback which helped to incorporate adaptation of the sensor allowing for sharp filtering and gain [13].

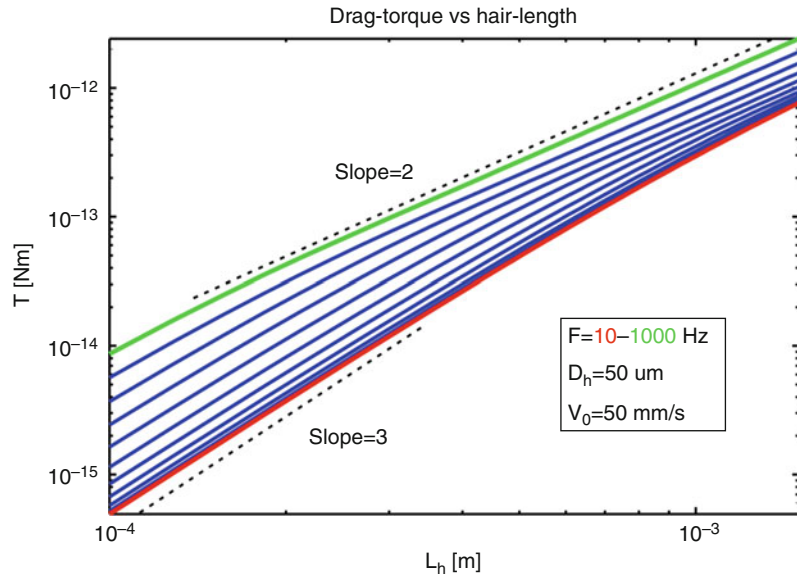
Hair-Sensor Systems for Operation in Air: A Case Study

Over the course of several years, the possibilities to fabricate hair-based flow sensors and sensor arrays inspired by the hair sensors and canopies as found on the cerci of crickets have been explored. In several sensor iterations, understanding optimization criteria alongside with viable and robust fabrication technology and suitable interfacing was targeted, not only for single hair sensors but also for arrays.

The scaling of the hair sensors is clearly confined by various requirements. First of all the sensors are supposed to capture a sufficient amount of drag-force. Evidently, the longer and thicker the hairs, the larger the drag torque is (see Fig. 2). Even more so since air flowing over a substrate forms a boundary layer in which the flow-velocity transitions from zero, at the substrate, to the maximum (far-field) value. This boundary layer depends on viscosity and becomes thinner with increasing frequency. Next, for given drag torque the angular rotation will increase when the rotational stiffness decreases. Hence, a small rotational stiffness will be beneficial for the sensitivity and flow-velocity threshold. However, animals live in dynamic environments in which the amount of information derived from the flow sensors not only depends on the sensors sensitivity but also on the bandwidth in which they are sufficiently sensitive. Combining these observations one finds, unfortunately, that this bandwidth goes down with the square-root of the ratio of the spring stiffness and moment of inertia. In order for the animals to capture a large amount of drag torque while still maintaining a low spring-stiffness at a usable large bandwidth, it turns out that long and thin hairs are beneficial. Parametric studies on the drag-force as modeled by Stokes' expressions showed that the dependence on hair diameter is far less than the dependence on hair length. Based on the mechanical

Biomimetic Flow Sensors,

Fig. 2 Viscous drag torque on a cylinder of length L_h , diameter of $50\ \mu\text{m}$ for various frequencies with flow amplitude of $10\ \text{mm/s}$



responsivity and available bandwidth, one can propose a figure of merit (FoM) given by:

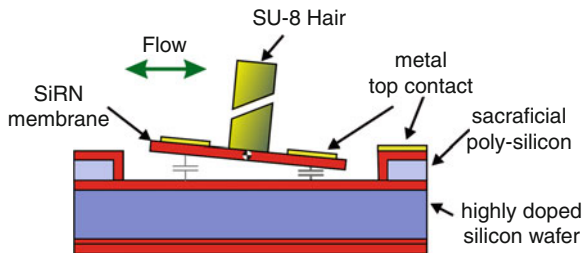
$$\frac{L^{1/2}}{\rho^{1/2} S^{1/2} D^{2/3}} \quad (1)$$

where L and D are the hair length and diameter, S is the rotational stiffness, and ρ is the specific mass density of the material from which the hairs are formed. The FoM is the product of the bandwidth of the sensors (expressed by the resonance frequency, i.e., square root of the rotational spring-stiffness S over the moment of inertia J) times their mechanical responsivity (i.e., the magnitude of angular rotation α per unit of flow-velocity V). Clearly it pays off to have long and thin hairs mounted on flexible suspensions.

The conditions under which hair sensors have to operate are such that the Reynolds (R) and Strouhal (St) numbers are relatively low. For a hair diameter of $25\text{--}50\ \mu\text{m}$, an air-oscillation frequency of $250\ \text{Hz}$ and a flow-velocity amplitude of $10\ \text{mm/s}$, R varies between 0.008 and 0.016 and St between 1.96 and 3.92 (for the flow around the hairs). The rather small Reynolds numbers and the large hair-length to hair-diameter ratio allow using the Stokes expressions for the drag torque exerted by the airflow on the hairs. Furthermore, these hair sensors are mounted on flat substrates allowing the use of the Stokes expressions for a harmonic flow along the hairs. These expressions

predict a viscous flow over an infinite substrate to be harmonic in time with zero flow velocity and 45° phase advance at the substrate interface and a boundary layer thickness (δ_b) proportional to the inverse of $\beta = (\omega/2\nu)^{0.5}$ where ν is the kinematic viscosity ($1.79 \cdot 10^{-5}\ \text{m}^2/\text{s}$ for air at room temperature) and ω is the radial frequency. The Stokes expressions can be usefully employed for this situation [7]. As an example, for a harmonic airflow of $100\ \text{Hz}$, the boundary layer is roughly $0.5\ \text{mm}$. Note that under most conditions the artificial hairs can be assumed infinitely stiff and the rotation angles are rather small (in the order of $1\text{--}100\ \text{mrad}$ amplitude per m/s flow-velocity amplitude).

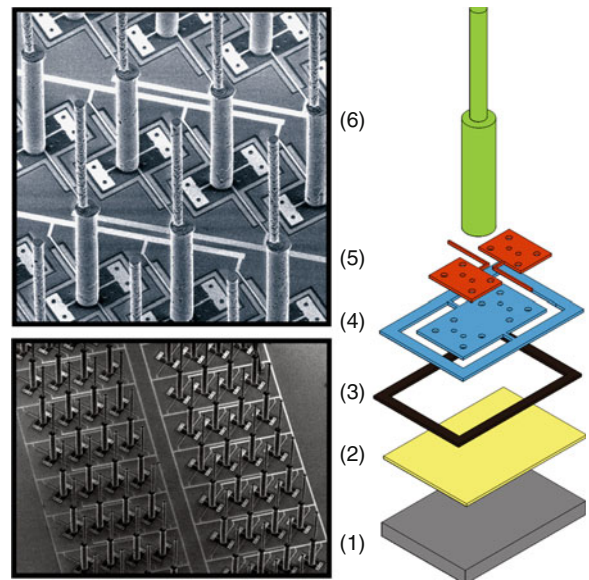
On a basal level the simple principle of a hair sitting on a torsional mount allowing for drag-induced rotation has been the starting point for these artificial hair sensors (see Fig. 3). In the implementation, the hairs are made of SU-8. Using two deposition-exposure cycles and subsequent development, these hairs can be made up to $1\ \text{mm}$ long with diameters of about $50\ \mu\text{m}$ for the bottom part and $25\ \mu\text{m}$ for the top part. This configuration hardly reduces the drag torque but decreases the moment of inertia of the artificial hairs by about 65% . The rotational freedom comes from two torsion beams. These beams as well as two membranes connected to the beams are made of silicon nitride. On the membranes an Al layer is deposited which forms a capacitor together with the underlying highly doped



Biomimetic Flow Sensors, Fig. 3 Schematic of artificial hair-based flow sensor with differential capacitive layout

silicon substrate. On drag-induced tilting of hair and membranes, the capacitances change in opposite fashion allowing for a differential capacitive read-out scheme. The hairs sit on the membranes as well. Rotational freedom is obtained when the structure is released by sacrificial etching of the poly-silicon layer ($0.5\text{--}1.0\ \mu\text{m}$ thick) that sits between the membrane and a protective silicon-nitride layer on the silicon substrate.

The choice for capacitive transduction is motivated by the fact that differential capacitive readout can be very sensitive and allows for rejection of various common mode signals (e.g., those that originate from flow in the direction perpendicular to the plane in which the hair is supposed to tilt). Moreover, contrary to e.g., thermal readout, it requires little power and does not thermally pollute the air around the sensors. This may not be important for a single hair but since the interest is in larger arrays, thermal effects could be far from negligible. Additionally capacitive readout allows for interrogation of many hair sensors in an array by frequency division multiplexing. There are also some clear drawbacks: the electronics required for capacitive readout are far more complex, certainly when compared to piezoresistive transduction and the method asks for rather complex mechanical structures when applied to sensors for use in liquids, especially in water. In the latter situation, the volume between the electrodes is ideally sealed in order to prevent liquid to get between since this could lead to electrolysis and large viscous damping. Figure 4 shows an exploded view of these capacitive, artificial hair-based flow sensors. Measurements of these sensors are shown in Fig. 5. Due to a combination of the boundary layer effect (high pass) and the second-order mechanics (i.e., its behavior is described by a second-order ordinary differential equation acting as low pass), the sensors show a band-pass characteristic.



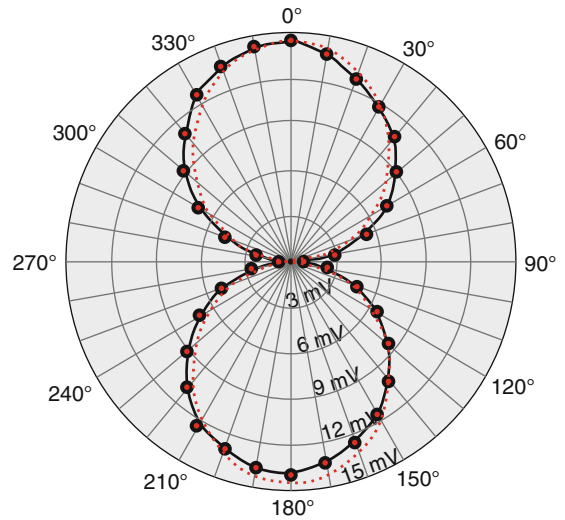
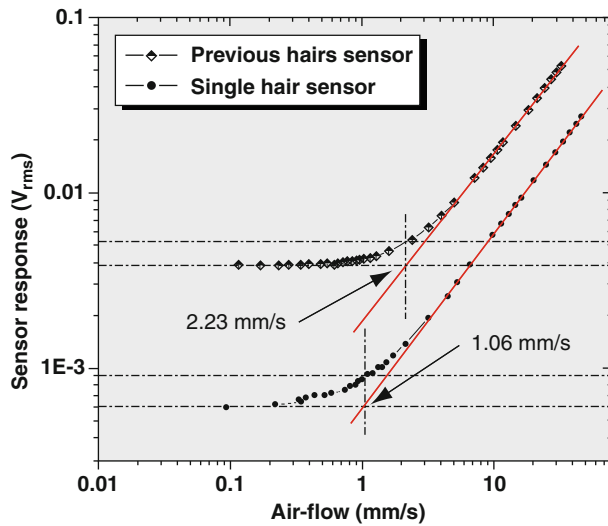
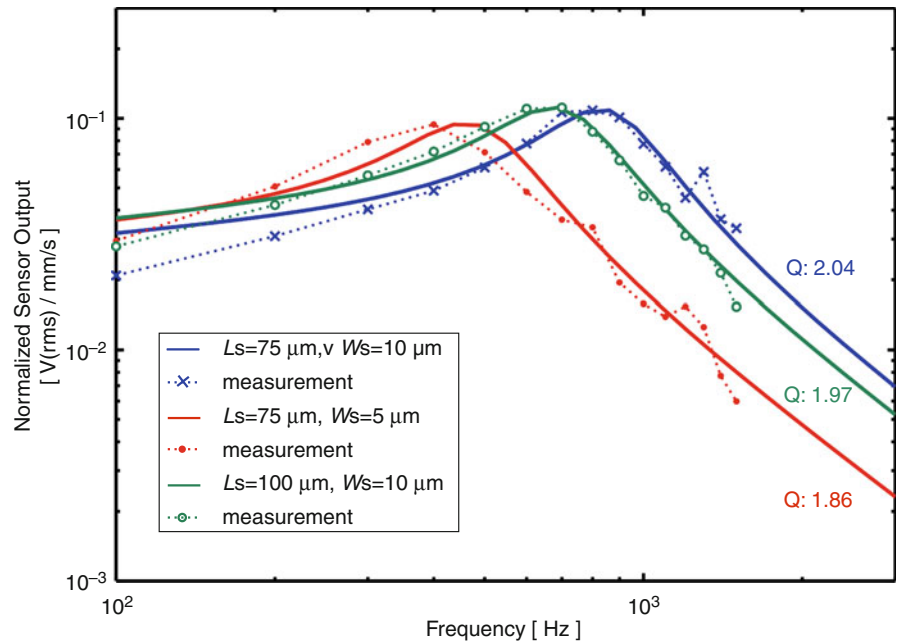
Biomimetic Flow Sensors, Fig. 4 Right: Exploded design view of a single hair sensor showing: (1) highly conductive silicon bulk (*bottom* electrode), (2) 200 nm thick SiRN layer for insulation and etch-stop, (3) Poly-silicon layer after final sacrificial etching, (4) 1 μm thick SiRN layer patterned into membranes, (5) 100 nm thick aluminum for *top* electrodes and (6) two 450 μm thick SU-8 layers patterned into a long hair. Left: SEM images of microfabricated hair sensor arrays with zoom of the two-stage artificial hairs

The beauty of the neural system lies in its robustness as well as its largely localized generation of signals. In contrast, the capacitive measurement method employed in these sensors is plagued by parasitic capacitances that can hardly be avoided and have a far less localized nature. Changes in temperature, humidity, wiring geometry, etc. indeed cause fluctuations of the parasitics which are large relative to the small capacitive changes that the hair sensors induce. Therefore, control of the parasitics is of paramount importance for a proper device functioning. A reduction in parasitics can be obtained using much smaller electrode areas as well as exploiting shielding. Both have been shown to be feasible using silicon-on-insulator (SOI) technology. Results of the latest generation of sensors are shown in Fig. 6.

Successive iterations led to airflow sensors delivering sensitivities of about $400\ \mu\text{m/s}$ (300 Hz bandwidth) with near-perfect figure of eight directivity. In order to do this, segmented cylinders, each up to 1 mm long, were used. Large arrays of sensors (over 100) can

Biomimetic Flow Sensors,

Fig. 5 Root mean square sensor output voltage normalized to 1 mm/s flow amplitude versus frequency for three sensor designs. *Solid lines* are model predictions, *symbols* measured responses. The values of the rotation beam length L_s and beam width W_s are indicated. The model predictions include fitted quality factors (Q) of 2.04 (blue line), 1.97 (green line), and 1.86 (red line) (Jaganatharaja et al. in preparation [11])



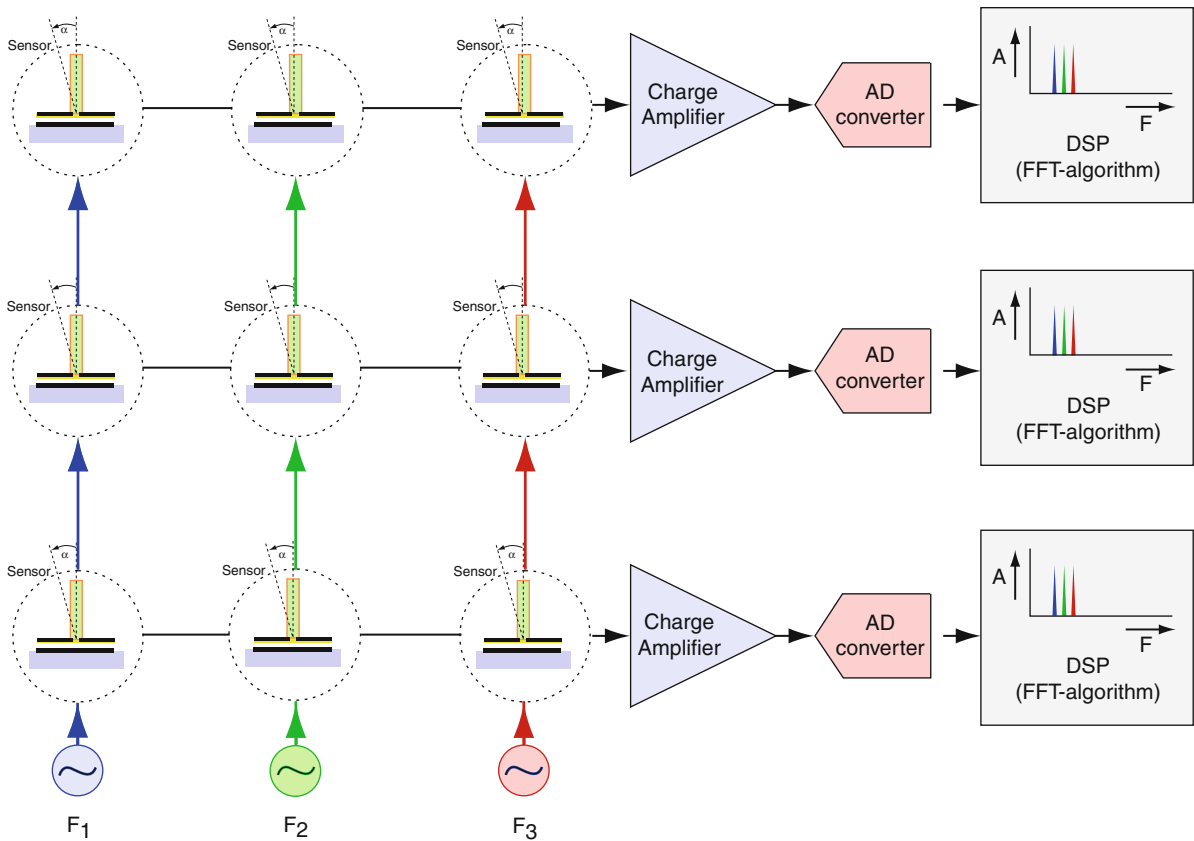
Biomimetic Flow Sensors, Fig. 6 *Left:* Output voltage of two generations of sensors measured in a 3 KHz bandwidth. The single hairs sensor is fabricated using a silicon on insulator substrate with a technology slightly different from the one indicated in Fig. 3. Measurements were done as a function of

flow-amplitude for a 250 Hz sinusoidal flow. *Red lines* are asymptotic lines to determine the threshold flow. *Right:* directivity of the single hair sensor showing an almost ideal figure of eight (*red dashed lines*)

be fabricated and, utilizing frequency division multiplexing, these sensors can be simultaneously and individually interrogated (see Fig. 7). This allows one to carry out measurements of spatiotemporal flow-patterns rather than single point measurements. Hence

the aim is to develop a system delivering the functionality of a “flow camera” with sensor densities of about 25–100 sensors per mm² [6]. This development has largely benefitted from insights in the cricket cercal system.

B



Biomimetic Flow Sensors, Fig. 7 Schematic of frequency division multiplexing as applied to hair-sensor array interfacing

Biomimetic Hairs in Water

Though functionally not necessarily different, hair-based flow sensors in water are confronted with some different scaling than sensors meant for air. The differences arise due to the fact that water has a higher mass density (about 1,000 times) and a smaller kinematic viscosity (about 20 times smaller). The first means that the effects of the moment of inertia of the hairs are smaller whereas the latter translates into boundary layers about 4.5 times smaller in water than in air. Hence, hairs for use in water can be both shorter and larger in diameter.

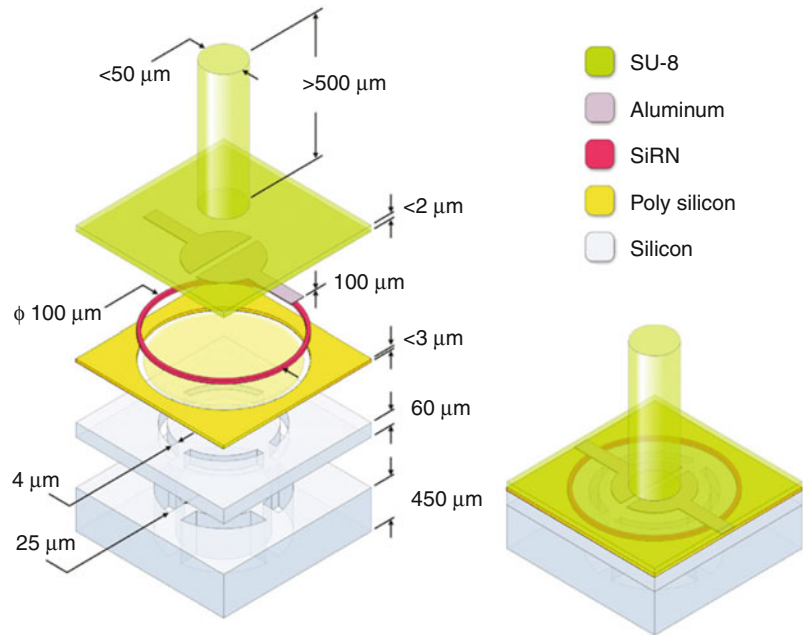
Hair-based sensing in water may exploit arbitrary transduction principles. However, the practical problems associated with capacitive readout caused by large viscous damping and necessary prevention of electrolysis may call for rather complicated technologies [9], as indicated in Fig. 8. This may be one of the

reasons that up to now not much work has been presented on capacitive aquatic hair-based sensors.

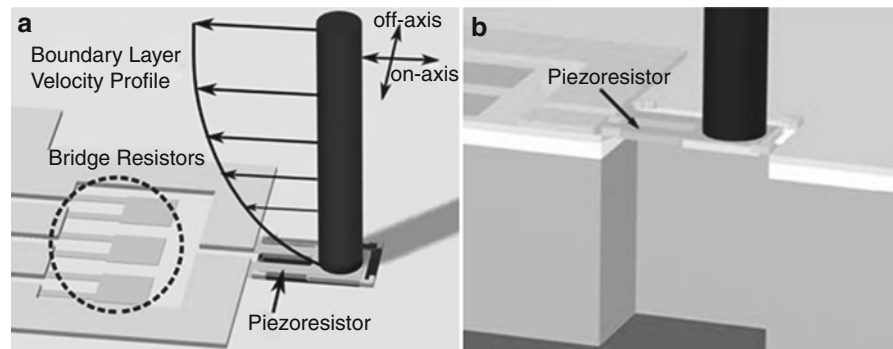
The piezoresistance-based artificial hair cell device, shown schematically in Fig. 9, consists of a cilium located at the distal end of a paddle-shaped silicon cantilever [5]. Doped silicon strain gauges are located at the base of the cantilever. The cilium is made of photodefinable SU-8 epoxy and is considered rigid. Lateral force along the on-axis acting on the cilium will create a bending moment (M), which is translated to the silicon beam through the stiff joint. The torque introduces a longitudinal strain and can be detected by piezoresistors at the base. The relation between the induced strain (ε) and the moment is given by

$$\varepsilon = \frac{6M}{Ewt^2} \quad (2)$$

Biomimetic Flow Sensors, Fig. 8 Exploded view of a capacitive aquatic hair-based flow sensor. The complex technology allows for sealed cavities (etched from the back side) safeguarding low damping and preventing electrolysis



Biomimetic Flow Sensors, Fig. 9 (a) Schematic drawing of an individual AHC sensor with superimposed boundary layer flow velocity profile. (b) Cross-sectional perspective view of the AHC

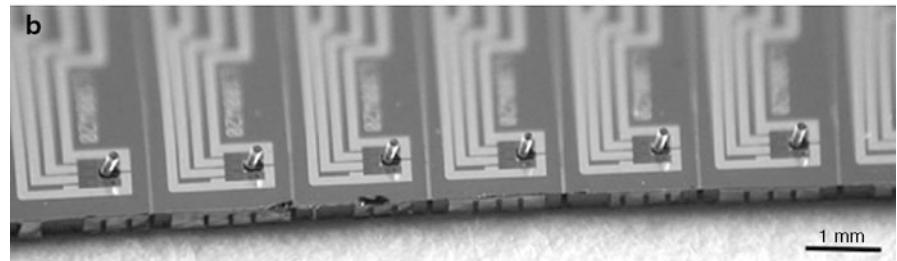
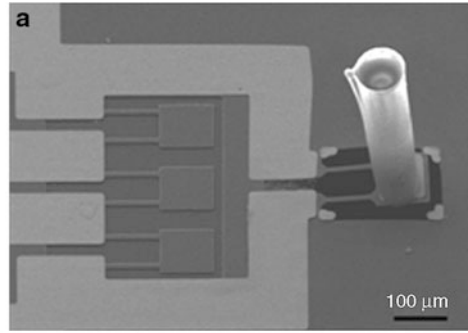
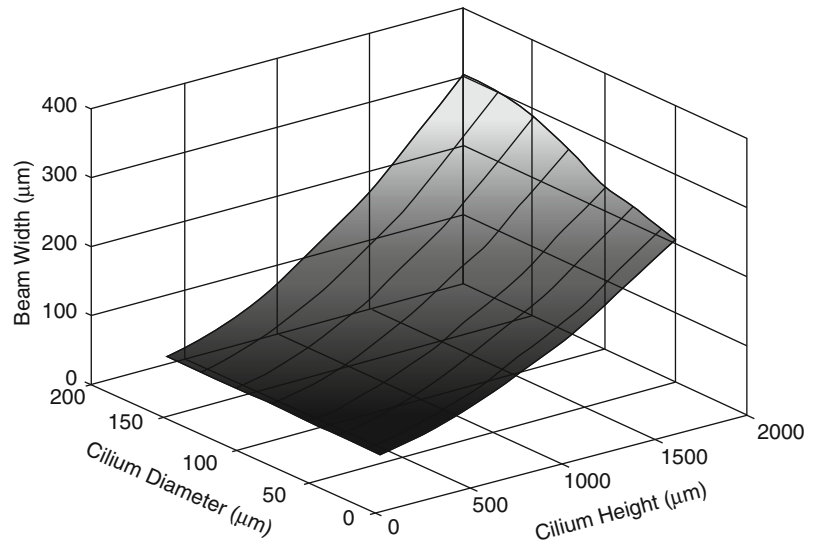


where E is the Young’s modulus of silicon, w the cantilever width, and t the cantilever thickness. When used as a flow sensor, flow passing along the cilium introduces a bending moment (M) due to frictional and pressure drag. The device is primarily designed for underwater applications that require sensing of low-velocity and low-frequency flows. Structural and hydrodynamic model analyses suggest that the sensor’s sensitivity is mainly determined by the following parameters: cantilever width (w), cantilever thickness (t), cilium height (h), cilium diameter (d), and sensor’s distance from the leading edge (x).

For real-life underwater applications, good sensitivity in the sub-1 mm/s flow velocity range is desirable. Based on the existing signal conditioning circuitry

capability, one can assume the minimum reliable voltage reading at 1,000 times signal gain as 1 mV. Taking 70 as a reasonable estimate for the gauge factor value, 1 mV output at 1,000 times signal gain translates into approximately 0.06 micro-strain using the quarter bridge model. In order to create and detect 0.06 micro-strain under 1 mm/s flow, the values of w , h , and d need to be carefully chosen. Figure 10 is a 3-D map with x , y , and z -axis being the three pertinent design variables, w , h , and d , respectively. A point within the plotted plane indicates a cantilever design that will satisfy the sensitivity requirement. The choice of w , h , and d are further narrowed down according to processing capabilities and frequency response considerations.

Biomimetic Flow Sensors,
Fig. 10 3-D map showing the possible combinations of cilium height, diameter, and cantilever width that satisfy the design requirements

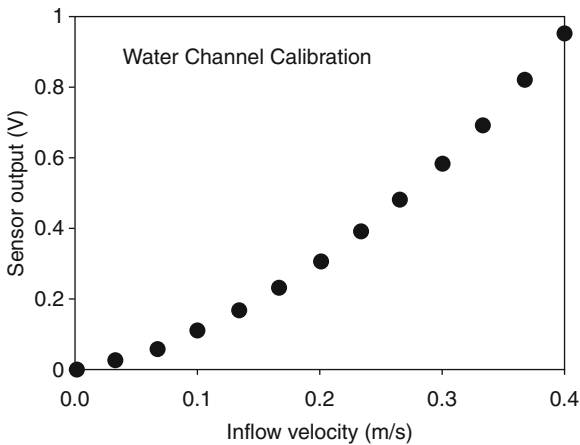


Biomimetic Flow Sensors,
Fig. 11 Scanning electron micrograph of (a) an individual and of (b) an array of AHC sensors

The cantilever thickness is chosen as $2\ \mu\text{m}$; this correlates to the thickness of the single crystal silicon epitaxial layer on the silicon-on-insulator (SOI) wafer used. For the analysis at hand, the sensor's distance from the leading edge (x) is assumed to be $2\ \text{mm}$, set by the die size. The devices are fabricated on SOI wafers with a $2\ \mu\text{m}$ thick epitaxial silicon layer on top, $2\ \mu\text{m}$ thick oxide, and $300\ \mu\text{m}$ thick handle wafer. SU-8 epoxy is chosen for its ability to form rigid high aspect ratio structures. Figure 11 shows an SEM of an actual device, and an array of AHC sensors. A series of

mechanical and electrical experiments were performed to characterize the sensor performance. The steady-state response to flow in water is presented in Fig. 12.

The sensitivity of artificial hair sensors can be tailored up to some extent. However, as indicated by the FoM above there is a trade-off between bandwidth and sensitivity. There seem to be some indications that nature does not only, or not per se, maximize the mechanical response (e.g., the rotational displacement of the hairs) but also optimizes the energy captured from the environmental flow. The allometric scaling of



Biomimetic Flow Sensors, Fig. 12 Experimental data of underwater steady-state flow velocity calibration of a single hair

cricket hairs seems to reflect the principle of mechanical impedance matching [19]. One may reason that capturing the maximum amount of energy will lead to the best signal-to-noise ratio whereas a high sensitivity may be obtained by proper adaptations, e.g., the lever ratio in the cricket hair-sensor system. Such systems are found more often in nature; for example, the middle ear of the mammalian hearing system is merely an impedance transformer. It offsets the impedance difference by a factor of a few tens in order to capture maximum energy from air-borne sound waves and convert it to traveling waves in the cochlea despite a factor of a few thousand difference in acoustic impedance. Up to date little has been done in artificial hair sensors to address this aspect. Nevertheless some studies have shown the possibility to improve sensor performance by properly covering the sensory hairs by hydrogel structures, as discussed above. The high water content, reminiscent of the cupular material found in fish neuromast, alleviates the mechanical impedance difference, which together with the increased hydrodynamic surface, leads to a 40-fold improvement in responsivity [18, 21].

Perspectives

The performance of single flow detecting biomimetic MEMS hairs has steadily improved over the last two decades and the threshold flow velocity is now only about one order of magnitude higher than for the most spectacular biological sensors. This is quite an

achievement, given that the signal transduction aspect of it is not carried out in a biomimetic approach. Some clever ideas might however originate from biology in this respect too. While active sensing, now found not only in humans and vertebrates but also in insects, has never been reported in these hairs yet, stochastic resonance has been already observed. This ability of biological systems to harness background or within-cell noise in order to improve signal capture needs to be seriously considered. Another as yet untapped possibility for increasing sensitivity and pattern recognition lies in the relative positioning of MEMS hairs, exploiting positive and negative viscous coupling [4]. Major challenges exist on the road until such sensors will be ready to use. They are brittle and break easily, in contrast to their natural counter parts which sustain very large deformations without harm. Furthermore, stiction problems (static friction) at the MEMS hair basis are occurring as soon as the flow velocity is too high, asking for incorporation of anti-stiction measures such as bumps and adhesion-reducing coatings. Nature is here again surprisingly resilient to extremes. Beyond potential technological applications, these hairs can now finally be turned into excellent physical models to tackle biological questions too difficult to address directly on biological materials: for example, the hydrodynamical interactions of tandem hairs moving within the same plane is nearly impossible to measure on real crickets, while MEMS of different lengths can be arranged at will.

Hair-based flow sensing is one of the few areas in which applied mathematics has been the common language of groups as diverse as field ecologists, materials scientists, aerodynamicists, theoretical physicists, computer scientists, and neurobiologists [3]. The mathematical toolbox, and its wide acceptance throughout the scientific community, is an unusual asset in biomimetics, as is the MEMS fabrication. Hair-based flow sensing is therefore *uniquely* suited for interactions among biologists and engineers working toward bio-inspired technologies.

Acknowledgments Without the many discussions we have had with our colleagues in the Cicada and Cilia projects this work would never have had the depth and breadth we have attained. These projects were the Cricket Inspired perCeption and Autonomous Decision Automata (CICADA) project (IST-2001-34718) and the Customized Intelligent Life Inspired Arrays (CILIA) project (FP6-IST-016039). Both projects were funded by the European Community under the Information Society Technologies (IST)

Program, Future and Emergent Technologies (FET), Lifelike Perception Systems action. We also like to acknowledge the contributions by our MSc and PhD students, PostDocs and technicians without which this paper would not exist.

Cross-References

- ▶ [Bio-inspired CMOS Cochlea](#)
- ▶ [Biosensors](#)
- ▶ [Integrated Micro-acoustic Devices](#)
- ▶ [Micro/Nano Flow Characterization Techniques](#)
- ▶ [Nanomechanical Resonant Sensors and Fluid Interactions](#)

References

1. Argyrakis, P., Hamilton, A., Webb, B., Zhang, Y., Gonos, T., Cheung, R.: Fabrication and characterization of a wind sensor for integration with a neuron circuit. *Microelectron. Eng.* **84**, 1749–1753 (2007)
2. Bleckmann, H., Zelick, R.: Lateral line system of fish. *Integr. Zool.* **4**, 13–25 (2009)
3. Casas, J., Dangles, O.: Physical ecology of fluid flow sensing in arthropods. *Annu. Rev. Entomol.* **55**, 505–520 (2010)
4. Casas, J., Steinmann, T., Krijnen, G.: Why do insects have such a high density of flow-sensing hairs? Insights from the hydromechanics of biomimetic MEMS sensors. *J. R. Soc. Interface* **7**, 1487–1495 (2010)
5. Chen, J., Fan, Z., Zou, J., Engel, J., Liu, C.: Two dimensional micromachined flow sensor array for fluid mechanics studies. *ASCE J. Aerosp. Eng.* **16**, 85–97 (2003)
6. Dagamseh, A., Bruinink, C., Kolster, M., Wiegerink, R., Lammerink, T., Krijnen, G.: Array of biomimetic hair sensor dedicated for flow pattern recognition. *Proc. DTIP 2010*, 5–7 May 2010, Seville, ISBN: 978-2-35500-011-9
7. Dijkstra, M., van Baar, J., Wiegerink, R., Lammerink, T., de Boer, J., Krijnen, G.: Artificial sensory hairs based on the flow sensitive receptor hairs of crickets. *J. Micromech. Microeng.* **15**, S132–S138 (2005)
8. Humphrey, J.A., Barth, F.G.: Medium flow-sensing hairs: biomechanics and models. In: Casas, J., Simpson, S.J. (eds.) *Insect Mechanics and Control. Advances in Insect Physiology*, vol. 34, pp. 1–80. Elsevier, Amsterdam (2008)
9. Izadi, N., de Boer, M.J., Berenschot, J.W., Krijnen, G.J.M.: Fabrication of superficial neuromast inspired capacitive flow sensors. *J. Micromech. Microeng.* **20**, 085041 (2010)
10. Jacobs, G.A., Miller, J.P., Aldworth, Z.: Computational mechanisms of mechanosensory processing in the cricket. *J. Exp. Biol.* **211**, 1819–1828 (2008)
11. Jaganatharaja, R.K.: Cricket inspired flow-sensor arrays. PhD thesis, University of Twente., 2011, ISBN 978-90-365-3215-0, <http://dx.doi.org/10.3990/1.9789036532150>
12. Kao, I., Kumar, A., Binder, J.: Smart MEMS flow sensor: theoretical analysis and experimental characterization. *IEEE Sens. J.* **7**(5), 713–722 (2007)
13. Kim, H., Song, T., Kang-Hun, A.: Sharply tuned small force measurement with a biomimetic sensor. *Appl. Phys. Lett.* **98**, 013704 (2011)
14. Li, F., Liu, W., Stefanini, C., Dario, P.: A novel bioinspired PVDF micro/nano hair receptor for a robot sensing system. *Sensors* **10**, 994–1011 (2010)
15. Lien, V., Vollmer, F.: Microfluidic flow rate detection based on integrated optical fiber cantilever. *Lab on a Chip* **7**, 1352–1357 (2007)
16. Mulder-Rosi, J., Cummins, G.I., Miller, J.P.: The cricket cercal system implements delay-line processing. *J. Neurophysiol.* **103**(4), 1823–1832 (2010)
17. Ozaki, Y., Ohyama, T., Yasuda T., Shimoyama I.: An air flow sensor modeled on wind receptor hair of insects. Presented at International Conference on MEMS, Miyazaki, 2000
18. Peleshanko, S., Julian, M.D., Ornatska, M., McConney, M.E., LeMieux, M.C., Chen, N., Tucker, C., Yang, Y., Liu, C., Humphrey, J.A.C., Tsukruk, V.V.: Hydrogel-encapsulated microfabricated haircells mimicking fish cupula neuromast. *Adv. Mater.* (19), 2903–2909 (2007).
19. Shimozawa, T., Murakami, J., Kumagai, T.: Cricket wind receptors: thermal noise for the highest sensitivity known. In: Barth, F.G., Humphrey, J.A., Secomb, T.W. (eds.) *Sensors and Sensing in Biology and Engineering*, pp. 145–159. Springer, Berlin (2003)
20. Xueb, C., Chena, S., Zhanga, W., Zhanga, B.: Design, fabrication, and preliminary characterization of a novel MEMS bionic vector hydrophone. *Microelectron. J.* **38**, 1021–1026 (2007)
21. Yang, Y.C., Nguyen, N., Chen, N.N., Lockwood, M., Tucker, C., Hu, H., Bleckmann, H., Liu, C., Jones, D.L.: Artificial lateral line with biomimetic neuromasts to emulate fish sensing. *Bioinspir. Biomim.* **5**(1) (2010)
22. Zhou, Z., Liu, Zhi-wen: Biomimetic cilia based on MEMS technology. *J. Bion. Eng.* **5**, 358–365 (2008)

Biomimetic Infrared Detector

- ▶ [Insect Infrared Sensors](#)

Biomimetic Mosquito-Like Microneedles

Melur K. Ramasubramanian and Ranjeet Agarwala
Department of Mechanical & Aerospace Engineering,
North Carolina State University, Raleigh, NC, USA

Synonyms

[Bioinspired microneedles](#); [Biomimicked microneedles](#); [Bionic microneedles](#); [Mosquito fascicle inspired microneedles](#); [Nature inspired microneedle](#)